Biochemical and Biophysical Research Communications 824 (2026) 153970

Contents lists available at ScienceDirect

Biochemical and Biophysical Research Communications

journal homepage: www.elsevier.com/locate/ybbrc

The functional landscape of STK35 residues at single-amino-acid resolution in the DNA damage response and genotoxic drug vulnerability

Zhixuan Zhang, Yangfang Xiong, Qian Pan *, Wensheng Wei **

Biomedical Pioneering Innovation Center, Beijing Advanced Innovation Center for Genomics, Peking–Tsinghua Center for Life Sciences, Peking University Genome Editing Research Center, State Key Laboratory of Protein and Plant Gene Research, School of Life Sciences, Peking University, Beijing, 100871, China

ARTICLE INFO

Keywords:
STK35
DNA damage response
Saturated base editing screen
Functional variant mapping
Genotoxic drug vulnerability

ABSTRACT

Maintaining genomic stability under genotoxic stress is crucial, yet many regulatory proteins within the DNA damage response (DDR) network remain functionally uncharacterized. Here, we identify the serine/threonine kinase STK35 as a broad regulator of the DDR. Depletion of STK35 significantly sensitizes diverse human cell lines to DNA-damaging agents, particularly DNA adduct-forming agents, including cisplatin and methyl methanesulfonate (MMS). Using systematic saturated adenine base editor (ABE) and cytosine base editor (CBE) screens, we performed saturated mutagenesis mapping of STK35, circumventing the limitations of traditional gene knockout approaches to resolve functionally critical residues at single-amino-acid resolution. This approach identified specific residues of STK35 within its conserved kinase domain, notably A423 and W445, whose mutations markedly sensitized cells to multiple DNA-damaging agents. We also identify SCP4 phenocopies STK35 loss under cisplatin and MMS treatment. Collectively, our findings establish STK35 as a broad DDR regulator and identify the functional landscape of STK35 through base-editing saturated screening,suggesting specific functional critical residues as potential targets for genotoxic drug vulnerability.

1. Introduction

Maintaining genomic stability is essential for cellular survival and disease prevention, including cancer [1,2]. The DNA damage response (DDR) is a highly coordinated signaling network that detects and repairs lesions induced by genotoxic stresses, including chemotherapeutic agents like cisplatin [3,4]. While core DDR pathways have been extensively characterized, identifying novel regulatory factors remains critical for elucidating therapeutic mechanisms and overcoming clinical drug resistance. Recent advances in high-throughput RNA interference and CRISPR-Cas9 screens have significantly facilitated the mapping of complex DDR networks [5–7]; nevertheless, many regulatory proteins—particularly kinases that fine-tune these stress responses—await detailed functional characterization.

STK35 (Serine/Threonine Kinase 35) belongs to the new kinase family 4 [8]. It has been implicated in actin dynamics, endothelial cell migration, and cell cycle progression [9], and is observed being upregulated in osteosarcoma and colorectal cancers [10,11]. However, its potential involvement in genomic stability remains unclear. In addition, recent work in acute myeloid leukemia (AML) identified *CTDSPL2*-encoded SCP4 as an upstream regulator of STK35, showing that SCP4 dephosphorylates inhibitory phosphorylation site (S385) on STK35 to support AML proliferation [12]. Our previous genome-wide base editor-mediated gene knockout screen identified STK35 as a novel factor upon cisplatin treatment [13]. Specifically, STK35 depletion sensitizes cells to cisplatin, promotes cell apoptosis and increases cell cycle G2/M phase arrest, accompanied by decreased levels of γH2AX and phosphorylation of ATM at S1981. These findings underscore a potentially broader role of STK35 in the DDR, prompting a systematic interrogation of its functional domains and amino acid residues.

Traditional gene-knockout approaches, while effective at validating gene essentiality, lack the resolution to decipher individual amino acid residues. To overcome this limitation, CRISPR-mediated base editors, including adenine and cytosine base editors (ABEs and CBEs), enable precise, endogenous nucleotide conversions without double-strand breaks [14,15]. This technology now support high-throughput, single--amino-acid resolution screening, to systematically map critical residues within proteins and signaling pathways [16–21], including recent functional annotation of DDR variants and genome maintenance mechanisms [22,23].

* Corresponding author.
** Corresponding author.
E-mail addresses: panqian@pku.edu.cn (Q. Pan), wswei@pku.edu.cn (W. Wei).

https://doi.org/10.1016/j.bbrc.2026.153970
Received 12 May 2026; Accepted 15 May 2026
Available online 16 May 2026

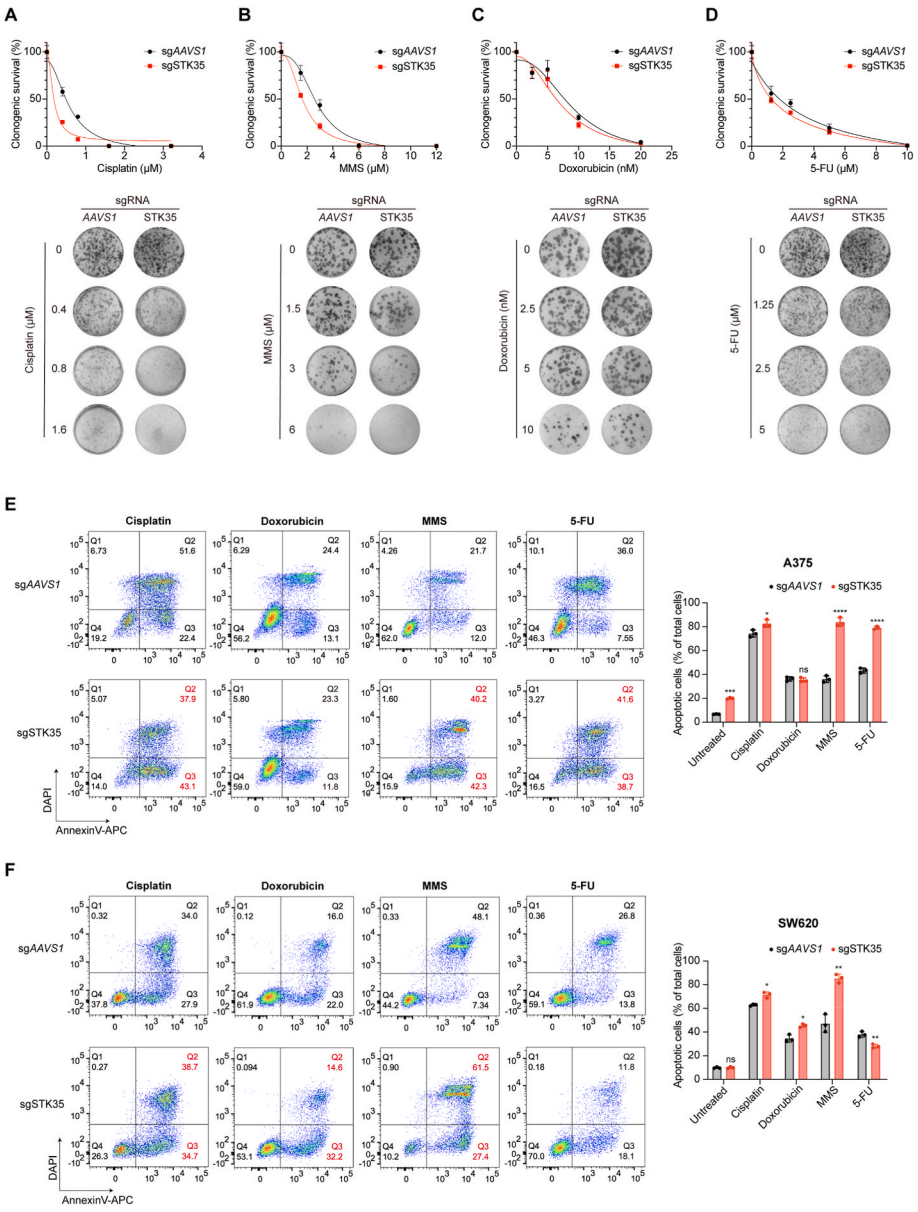

Fig. 1. STK35 deficiency sensitizes multiple cell lines to diverse DNA-damaging agents. (A-D) Clonogenic survival assay of STK35-knockout RPE1 cells under (A) cisplatin, (B) MMS, (C) doxorubicin and (D) 5-FU treatment. sg*AAVS1* served as the negative control. Quantification is displayed (top) with representative images (bottom). The 0 μM control image and data are shared between cisplatin and 5-FU panels, as experiments were performed concurrently. (E-F) Flow cytometric analysis (left) and quantification (right) of Annexin V-*positive* apoptotic A375 and SW620 cells. Data: mean ± SD; n = 3; unpaired two-tailed Student's t-test (*p < 0.05, **p < 0.01, ***p < 0.001, ****p < 0.0001; ns, not significant).

In this study, we demonstrated STK35 as a broad DDR regulator across multiple cell lines responding to diverse genotoxic agents. Using base editing-mediated saturated mutagenesis spanning the entire gene, we systematically mapped critical residues required for its DDR function at the single-amino-acid resolution. This study provides the first genetic landscape of STK35, offering a valuable framework for interpreting clinical genetic variants and developing targeted therapeutic strategies.

2. Materials and methods

2.1. Plasmid construction

Individual sgRNA expression plasmids were constructed by annealing oligonucleotides and cloning into pCG2.0-sgRNA-mCherry/EGFP via Golden Gate (*Bsm*BI). ABEmax (Addgene #112101) or a synthesized AncBE4max [24] sequence were cloned into pLenti_P2A_EGFP/mCherry vectors using restriction digestion and ligation.

2.2. Cell culture and treatment

HEK293T and A375 cells were cultured in DMEM (Gibco), RPE1 cells in DMEM/F12 (Gibco), SW620 cells in RPMI 1640 (Gibco), supplemented with 10% fetal bovine serum and 1% penicillin/streptomycin, at 37 °C with 5% CO_2.

Cisplatin was from Selleck. MMS, doxorubicin, and 5-FU were from Sigma-Aldrich. PEI reagent (Proteintech) was used for plasmid transfection and lentiviral packaging.

2.3. Library construction

Oligonucleotides of ABE/CBE libraries were synthesized (Synbio Technologies) and ligated into the sgRNA expression vectors pCG2.0-

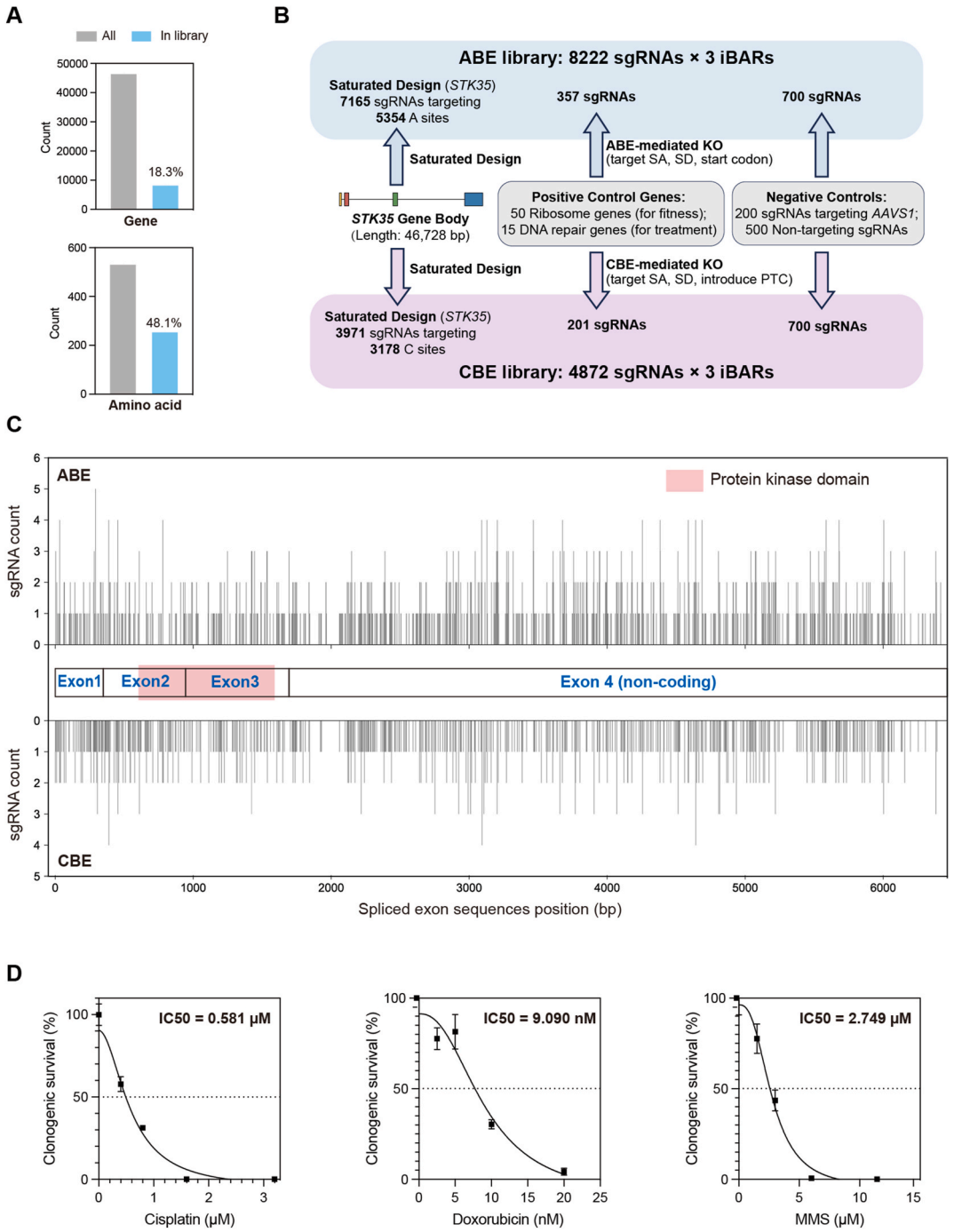

Fig. 2. Design and characterization of saturated STK35 ABE and CBE mutagenesis libraries. (A) STK35 library coverage. (B) sgRNA design principles. (C) Library sgRNA exon distributions (D) IC50 determination for cisplatin, doxorubicin, and MMS in RPE1 cells via clonogenic assays. Data: mean ± SD; n = 3.

sgRNA-mCherry/EGFP containing three distinct internal barcodes (iBARs: CTCGCT, GATGGT, and GCACTG) using Golden Gate cloning (*Bsm*BI). Utilizing our established iBAR strategy and corresponding data analysis method [25,26], we can perform credible screening at a high multiplicity of infection (MOI, ~3). Plasmid libraries were amplified into HST08 competent cells (Takara, #9028) and packaged into lentiviruses by co-transfecting HEK293T cells with pR8.74 and pVSVG. Supernatants were harvested 72 h post-transfection.

2.4. Lentiviral titration and infection

Viral titers were determined by transducing cells with serial dilutions of supernatant plus 8 μg/mL polybrene. Infection efficiency was assessed 48–72 h later via flow cytometry (for fluorescent markers) or CellTiter-Glo (for puromycin resistance) and viral volumes were calculated to achieve target MOI. Post-infection, media were replaced after 24 h, and subsequent assays were performed after 48–72 h.

2.5. Library screening

RPE1 cells expressing ABEmax or AncBE4max were infected with sgRNA libraries at MOI ~3. After puromycin selection (15 μg/mL), surviving cells were harvested as the Day 0 control. Remaining cells were divided into untreated and drug-treated (cisplatin, doxorubicin, or

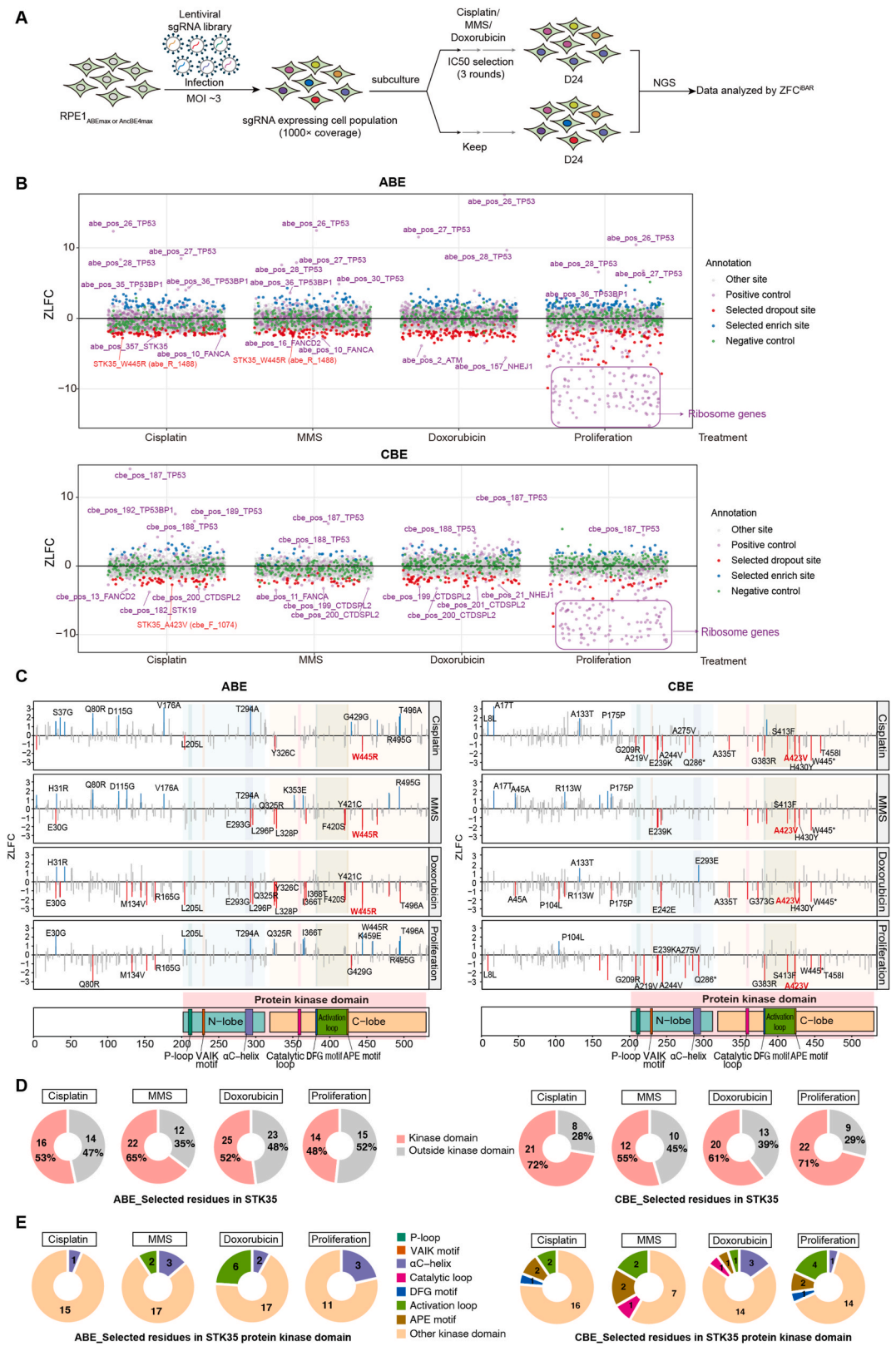

Fig. 3. Overview of STK35 saturated library screening. (A) Screening workflow. (B) Scatter plots showing z-score normalized log2 fold changes (zLFC) of sgRNAs across proliferation and drug-treated groups. (C) Positional mapping of functional hits across STK35 coding regions, with the kinase domain and conserve kinase motifs indicated. sgRNAs commonly enriched (blue) or depleted (red) in multiple conditions are highlighted. (D-E) Distribution of prioritized variants inside versus outside the kinase domain (E) and across conserved motifs (F). (For interpretation of the references to color in this figure legend, the reader is referred to the Web version of this article.)

MMS) groups. Cells were passaged every 3 days until Day 24, with drug pulses every 6 days. Genomic DNA was isolated (Qiagen), and integrated sgRNAs were amplified by PCR (Roche) for Next-Generation Sequencing.

2.6. Library data analysis

Library data analysis was performed using the previously published ZFC^{iBAR} analytical method [25]. This method uses the zLFC (z-score log fold change) to evaluate changes in sgRNA^{iBAR} abundance. For drug treatment, day 24 drug-treated groups were compared to day 24 untreated group; for proliferation, day 24 untreated group was compared to day 0.

2.7. Clonogenic survival assay

Twenty-four hours after seed*ing* in 6-well plates, *cells were* treated with drugs for 48 h, and then cultured for 7–14 days. Colonies were washed with PBS, fixed with anhydrous methanol and stained with 0.1% crystal violet solution (Solarbio).

2.8. Apoptosis analysis

After 48 h of drug treatment, cells were harvested, washed with PBS, double-stained with Annexin V-APC/DAPI (Procell), and analyzed via flow cytometry.

2.9. Cell proliferation assay in response to drug treatment

Individual sgRNAs were transduced into RPE1-ABEmax/AncBE4max single clone cells at MOI of ~0.7, to achieve ~50% initial fluorescence. Cells were passaged every three days and treated with cisplatin (0.8 μM) or MMS (3 μM) for 2 days. Following each treatment cycle, the percentage of fluorescent cells was analyzed via flow cytometry.

3. Results

3.1. STK35 acts as a broad DDR regulator across diverse genotoxic agents and cell lines

Our initial screening and validation in RPE1 cells demonstrated that STK35 depletion significantly sensitizes cells to cisplatin [13], confirming its involvement in the cellular response to cisplatin-induced DNA damage (Fig. 1A). To determine whether this function extends to other genotoxic stresses, we further evaluated cell viability under treatment with additional DNA-damaging agents: MMS (a DNA alkylating agent, Fig. 1B), Doxorubicin (a topoisomerase II inhibitor that primarily induces DNA strand breaks, Fig. 1C), and 5-Fluorouracil (5-FU; a pyrimidine analog that inhibits thymidylate synthase, Fig. 1D).

As shown in Fig. 1A–D, STK35 deficiency increased cellular sensitivity to all four agents, most strongly to cisplatin and MMS, both of which primarily induce DNA adduct-associated damage. These results suggest that STK35 is broadly involved in the DDR, with a potential preference for DNA crosslink and alkylation damage response pathways.

To further assess the generality of this phenotype, we extended to cancer cell lines, A375 and SW620. Apoptosis assays revealed that STK35 depletion consistently heightened sensitivity to cisplatin and MMS across these diverse genetic backgrounds. However, the impact on doxorubicin and 5-FU sensitivity showed cell-line-specific variations (Fig. 1E and F).

Taken together, these data establish STK35 as a critical DDR regulator, with a particularly robust role in mitigating DNA adduct damage induced by cisplatin and MMS. These observations warrant further investigation of the specific functional residues that govern this activity.

3.2. Design of saturated ABE and CBE libraries targeting STK35

To identify DDR-relevant STK35 residues, we designed saturated mutagenesis libraries using ABE and CBE. After PAM compatibility and off-target sgRNA filtering, our ABE and CBE libraries covered approximately 18.3% of all nucleotides across the whole STK35 gene body and 48.1% of its coding sequence (Fig. 2A). Specifically, the ABE library comprised 7165 sgRNAs targeting 5354 adenosines, while the CBE library included 3971 sgRNAs targeting 3178 cytidines (Fig. 2B).

The libraries incorporated two categories of positive controls: 50 essential ribosomal genes to monitor cell proliferation and 15 previously reported DDR-related genes to evaluate drug response. For the ABE library, we targeted adenines in the splice acceptor (SA) and splice donor (SD) sites, as well as the start codon (ATG), to induce gene disruption, consistent with previous established methods [27,28]. For the CBE library, sgRNAs were designed to target cytidines in SA/SD sites or introduce premature termination codons (PTCs), to induce gene disruption, following prior methodologies [25,29,30]. Negative controls consisted of 200 sgRNAs targeting the *AAVS1* safe-harbor locus and 500 non-targeting sgRNAs.

STK35 consists of four exons and contains a conserved protein kinase domain. The distribution and coverage of ABE/CBE sgRNAs across the STK35 exons are illustrated in Fig. 2C. Based on our preliminary results, we selected three genotoxic agents—cisplatin, doxorubicin, and MMS—for the screening. To identify mutations conferring either sensitization or resistance, we utilized the IC50 dose determined in RPE1 cells *(*Fig. 2D*)* of each drug for subsequent functional screening.

3.3. Systematic mapping of STK35 functional residues via saturated base editing screens

The screening workflow is delineated in Fig. 3A. We first established RPE1 cell lines stably expressing optimized base editors, ABEmax and AncBE4max [24]. Following lentiviral transduction of the sgRNA libraries, cells were cultured and subjected to three rounds of treatment with cisplatin, doxorubicin, or MMS at their respective IC50 dosages. Genomic DNA was harvested on day 24, and sgRNA abundance was analyzed using untreated cells as controls. The cell proliferation group was analyzed at day 24 normalized to day 0 population.

The screening results for the ABE and CBE libraries, including the cell proliferation group, exhibited distributions consistent with experimental expectations (Fig. 3B). Notably, top-ranked enriched sgRNAs under drug treatment were predominantly mapped to the positive control, essential regions of *TP53*, consistent with its well-established role in DNA damage-induced growth arrest [31]. Conversely, significantly depleted sgRNAs included multiple known DDR factors as well as novel candidate sites within STK35. For instance, FANCA and FANCD2, core components of the Fanconi anemia pathway involved in interstrand crosslink repair [32], were significantly depleted in the cisplatin and MMS groups. In the doxorubicin group, NHEJ1, a key factor in non-homologous end joining (NHEJ) pathway responding to DNA double strand breaks [33], was identified as a major dropout hit. In the proliferation group, the top depleted hits were almost exclusively confined to the positive control ribosomal genes, further supporting the technical robustness of the screening.

Focusing specifically on the STK35 coding region (Fig. 3C), sgRNAs associated with significant phenotypes across multiple treatment groups are highlighted in red (depletion) and blue (enrichment). To better summarize the functional landscape, we annotated the STK35 domain architecture and conserved kinase motifs, and quantified the distribution of candidate variants inside versus outside the kinase domain (Fig. 3D), as well as within conserved kinase motifs (Fig. 3E). These analyses revealed variants enrichment within or near conserved kinase domain and canonical motifs. This positional enrichment, especially the recurrent sites across different drug groups, likely impair STK35 kinase-domain function. However, the presence of hits outside the kinase

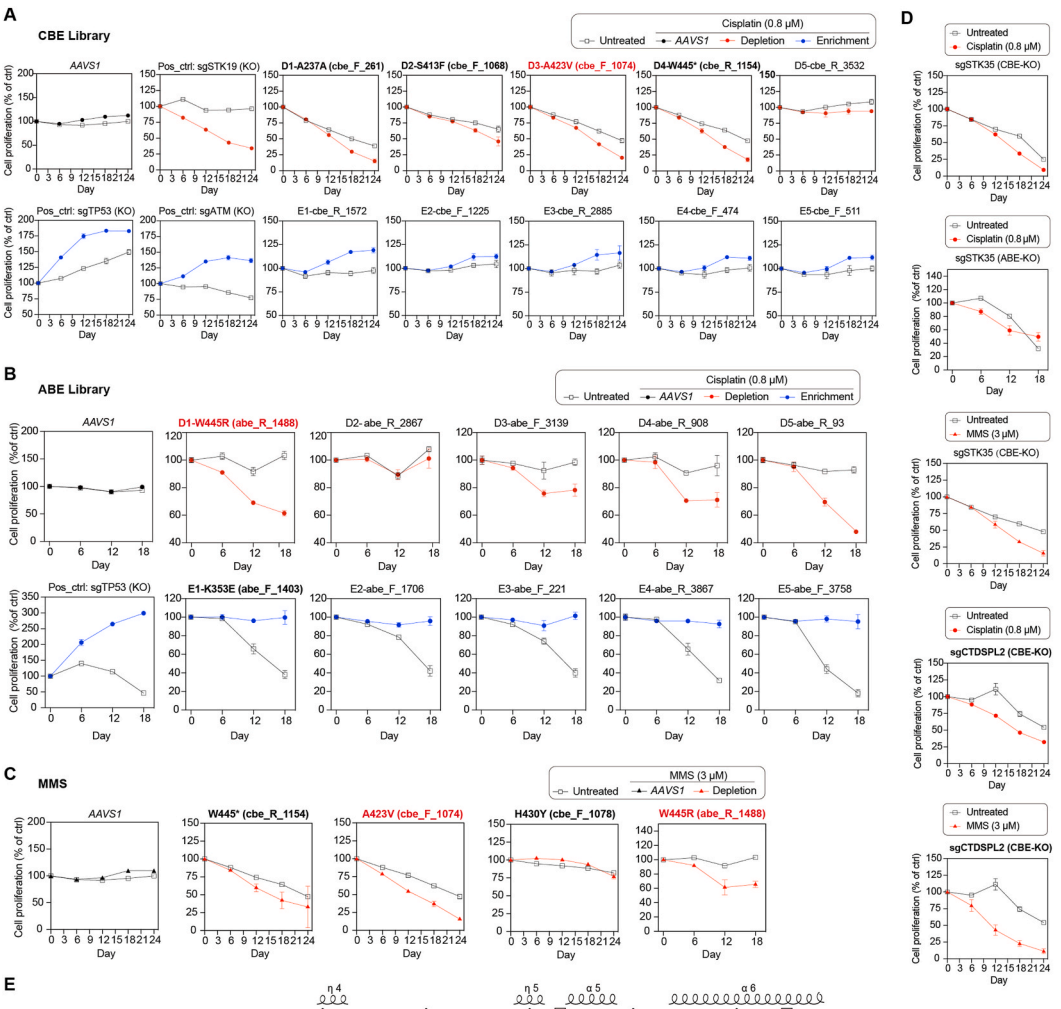

(caption on next page)

Fig. 4. Validation of STK35 functional residues and the SCP4-related phenotype. (A-B) Individual sgRNA validation of top-ranked variants from CBE (A) and ABE (B) libraries under cisplatin treatment. Bold text denotes sgRNAs targeting coding regions. (C) MMS sensitivity validation for common hits identified across multiple drug-screening groups. (D) Proliferation assays of cells transduced with sgRNAs targeting *STK35* and *CTDSPL2* gene knockout under cisplatin and MMS treatment. Data: mean ± SD; n = 3. (E-F) Sequence alignment of STK35 orthologs across different species (E) and conserved catalytic core alignment of STK35 with representative human kinases (F). Strictly conserved residues: red background; Similar residues: red font; Secondary structure of human STK35 above the sequences (α: α-helices; η: 3_{10}-helices). (G) Structural modeling of STK35 kinase domain and identified mutation sites. Insets show close-up comparisons between wild-type (WT) and mutant residues (A423V, W445R). (H) Hydrophobic pocket surrounding W445 (yellow sticks). (For interpretation of the references to color in this figure legend, the reader is referred to the Web version of this article.)

domain implies additional, non-canonical functional regions of STK35 in the DDR.

Overall, our saturated mutagenesis screen demonstrated high technical quality and provided a systematic functional annotation of the STK35 locus.

3.4. Identification of candidate functional amino acid residues of STK35 in DDR

To confirm the functional relevance of the candidates identified in our primary screen, we performed individual drug response assays of the most significant and consistent sites. Fig. 4A–B presents the responses of cells harboring the top five sgRNAs from the CBE and ABE libraries, respectively, under cisplatin treatment. Both positive controls and negative control (*AAVS1*) were included for comparison. Similarly, sites consistently identified in both cisplatin and MMS screens were also validated under MMS treatment (Fig. 4C). Most tested variants exhibited significant alterations in drug sensitivity, consistent with the primary screening data.

Notably, our results highlighted two candidate functional residues, A423 and W445, both located within the conserved kinase domain of STK35. Specifically, sgRNAs inducing the A423V and W445R mutations significantly sensitized cells to both cisplatin and MMS. Multiple-sequence alignment across STK35 orthologs showed that both residues are evolutionarily conserved (Fig. 4E). In addition, kinase-family alignment revealed that A423 is positioned within the canonical APE motif at the activation loop's C-terminal, a highly conserved kinase element stabilizing the activation-segment and catalytic conformation (Fig. 4F). Thus, the A423V substitution introducing a bulkier side chain likely perturbs local conformation and the catalytic motif geometry (Fig. 4G). By contrast, W445 is within a tightly packed hydrophobic environment in the kinase C-lobe (Fig. 4H), as predicted by AlphaFold2 (pLDDT > 90). Substituting this buried tryptophan with a positive charged arginine is predicted to be structurally unfavorable and destabilizing, as supported by *in silico* tools (DUET, Missense3D, and DynaMut2). Together, these data support the view that A423 in conserved kinase motif likely maintains activation-segment organization, whereas W445 is important for maintaining local structural integrity of the kinase domain.

Consistent with our initial findings, the complete knockout of STK35 also enhanced drug sensitivity (Fig. 4D). Interestingly, *CTDSPL2* (encoding the SCP4 protein), which was included in our positive control panel, emerged as a top hit in our screen. SCP4 has been previously reported to be an upstream activation factor of STK35 in a distinct biological context, the AML proliferation [12]. Our validation suggested that *CTDSPL2* deficiency phenocopies STK35 deficiency in sensitizing cells to both cisplatin and MMS. These observations highlight a putative link between SCP4 and STK35 within the DDR framework, implying a role for this axis in genome maintenance that warrants further investigation.

4. Discussion

In this study, we systematically defined the functional landscape of STK35 in the DDR using high-throughput saturated base editing screens. While our previous studies have first associated STK35 with the DDR [13], this study unveils its broad necessity in surviving genotoxic stress. Notably, STK35 depletion profoundly sensitizes cells to cisplatin and MMS across diverse genetic backgrounds, suggesting a preferential involvement in the repair of DNA adducts and crosslinks.

A major technical advantage of our approach is utilizing saturated ABE and CBE libraries to achieve single-amino-acid resolution, overcoming the limitations of traditional CRISPR-Cas9 knockout screens that eliminate entire proteins and obscure distinct functional domains. By interrogating 48.1% of the amino acid residues, we identified specific variants conferring hypersensitivity rather than merely assessing gene essentiality. The high technical quality of our screen, evidenced by the expected behavior of positive controls and top-ranked candidates, validates the robustness of our functional annotations.

Notably, our validation indicates A423 and W445 as key residues within the kinase domain, whose mutation sensitizes cells to both cisplatin and MMS. Sequence and structural analyses provide a mechanistic framework: A423 is evolutionarily conserved within the canonical APE motif at the activation loop, essential for stabilizing activation-segment architecture and catalytic competent conformation; The A423V substitution, introducing a bulkier side chain, likely perturbs this constrained motif, impairing kinase-domain function. In contrast, W445 is buried in a hydrophobic region of the kinase C-lobe. Its substitution to a positive charged arginine (W445R), is predicted to disrupt local packing and destabilize the kinase domain. While biochemical studies are needed to confirm altered kinase activity or protein interactions, our data suggest that both residues are functionally important for maintaining the STK35 kinase domain integrity.

Our screen also linked the *CTDSPL2*-encoded SCP4 to the DDR, a previously reported upstream phosphatase of STK35 in AML cells [12]. The observation that SCP4 loss phenocopies STK35 deficiency under cisplatin and MMS treatment raises the possibility that this relationship may also be relevant in the genotoxic stress. However, as current study did not directly test this interaction in DDR or the impact of STK35 variants on SCP4 regulation, we currently interpret SCP4 here as a phenocopying factor and a candidate upstream regulator whose precise role in STK35-dependent genotoxic stress tolerance requires future mechanistic investigation.

From a translational perspective, our findings nominate STK35 as a potential modulator of tumor sensitivity to DNA-damaging agents. Identifying functionally important residues, like A423 and W445, provides starting points for future structure-guided drug discovery and mechanistic studies. Whether pharmacological inhibition of STK35, potentially in coordination with SCP4 modulation, can be exploited to enhance genotoxic therapy responses warrants substantial future investigation.

CRediT authorship contribution statement

Zhixuan Zhang: Data curation, Formal analysis, Investigation, Methodology, Validation, Visualization, Writing – original draft. **Yangfang Xiong:** Formal analysis, Software, Visualization. **Qian Pan:** Data curation, Formal analysis, Investigation, Methodology, Validation, Writing – review & editing. **Wensheng Wei:** Conceptualization, Funding acquisition, Project administration, Resources, Supervision.

Declaration of competing interest

The authors declare that they have no known competing financial

interests or personal relationships that could have appeared to influence the work reported in this paper.

Acknowledgements

This research was financially supported by the National Science Foundation of China (NSFC31930016), the Peking-Tsinghua Center for Life Sciences, and Changping Laboratory (to W.W.). We are grateful to Y. Sun (PKU) for supplying RPE1 cell line, the National Center for Protein Sciences (PKU) for their assistance with flow cytometry, and the technical support provided by PKU's High-performance Computing Platform.

References

[1] C.J. Lord, A. Ashworth, The DNA damage response and cancer therapy, Nature 481 (2012) 287–294, https://doi.org/10.1038/nature10760.
[2] S.P. Jackson, J. Bartek, The DNA-damage response in human biology and disease, Nature 461 (2009) 1071–1078, https://doi.org/10.1038/nature08467.
[3] A. Basu, S. Krishnamurthy, Cellular responses to cisplatin-induced DNA damage, J. Nucleic Acids 2010 (2010) 1–16, https://doi.org/10.4061/2010/201367.
[4] C. Rocha, M. Silva, A. Quinet, J. Cabral-Neto, C. Menck, DNA repair pathways and cisplatin resistance: an intimate relationship, Clinics 73 (2018), https://doi.org/10.6061/clinics/2018/e478s.
[5] M. Zimmermann, O. Murina, M.A.M. Reijns, A. Agathanggelou, R. Challis, Ž. Tarnauskaitė, M. Muir, A. Fluteau, M. Aregger, A. McEwan, W. Yuan, M. Clarke, M.B. Lambros, S. Paneesha, P. Moss, M. Chandrashekhar, S. Angers, J. Moffat, V. G. Brunton, T. Hart, J. de Bono, T. Stankovic, A.P. Jackson, D. Durocher, CRISPR screens identify genomic ribonucleotides as a source of PARP-trapping lesions, Nature 559 (2018) 285–289, https://doi.org/10.1038/s41586-018-0291-z.
[6] R.D. Paulsen, D.V. Soni, R. Wollman, A.T. Hahn, M.-C. Yee, A. Guan, J.A. Hesley, S. C. Miller, E.F. Cromwell, D.E. Solow-Cordero, T. Meyer, K.A. Cimprich, A genome-wide siRNA screen reveals diverse cellular processes and pathways that mediate genome stability, Mol. Cell 35 (2009) 228–239, https://doi.org/10.1016/j.molcel.2009.06.021.
[7] M. Olivieri, T. Cho, A. Álvarez-Quilón, K. Li, M.J. Schellenberg, M. Zimmermann, N. Hustedt, S.E. Rossi, S. Adam, H. Melo, A.M. Heijink, G. Sastre-Moreno, N. Moatti, R.K. Szilard, A. McEwan, A.K. Ling, A. Serrano-Benitez, T. Ubhi, S. Feng, J. Pawling, I. Delgado-Sainz, M.W. Ferguson, J.W. Dennis, G.W. Brown, F. Cortés-Ledesma, R.S. Williams, A. Martin, D. Xu, D. Durocher, A genetic map of the response to DNA damage in human cells, Cell 182 (2020) 481–496.e21, https://doi.org/10.1016/j.cell.2020.05.040.
[8] P. Goyal, A. Behring, A. Kumar, W. Siess, Identifying and characterizing a novel protein kinase STK35L1 and deciphering its orthologs and close-homologs in vertebrates, PLoS One 4 (2009) e6981, https://doi.org/10.1371/journal.pone.0006981.
[9] P. Goyal, A. Behring, A. Kumar, W. Siess, STK35L1 associates with nuclear actin and regulates cell cycle and migration of endothelial cells, PLoS One 6 (2011) e16249, https://doi.org/10.1371/journal.pone.0016249.
[10] H. Yang, J. Zhu, G. Wang, H. Liu, Y. Zhou, J. Qian, STK35 is ubiquitinated by NEDD4L and promotes glycolysis and inhibits apoptosis through regulating the AKT signaling pathway, influencing chemoresistance of colorectal cancer, Front. Cell Dev. Biol. 8 (2020) 582695, https://doi.org/10.3389/fcell.2020.582695.
[11] Z. Wu, J. Liu, S. Hu, Y. Zhu, S. Li, Serine/threonine kinase 35, a target gene of STAT3, regulates the proliferation and apoptosis of osteosarcoma cells, Cell. Physiol. Biochem. 45 (2018) 808–818, https://doi.org/10.1159/000487172.
[12] S.A. Polyanskaya, R.Y. Moreno, B. Lu, R. Feng, Y. Yao, S. Irani, O. Klingbeil, Z. Yang, Y. Wei, O.E. Demerdash, L.A. Benjamin, M.J. Weiss, Y.J. Zhang, C. R. Vakoc, SCP4-STK35/PDIK1L complex is a dual phospho-catalytic signaling dependency in acute myeloid leukemia, Cell Rep. 38 (2022) 110233, https://doi.org/10.1016/j.celrep.2021.110233.
[13] Q. Pan, Z. Zhang, Y. Xiong, Y. Bao, T. Chen, P. Xu, Z. Liu, H. Ma, Y. Yu, Z. Zhou, W. Wei, Mapping functional elements of the DNA damage response through base editor screens, Cell Rep. 43 (2024) 115047, https://doi.org/10.1016/j.celrep.2024.115047.
[14] A.C. Komor, Y.B. Kim, M.S. Packer, J.A. Zuris, D.R. Liu, Programmable editing of a target base in genomic DNA without double-stranded DNA cleavage, Nature 533 (2016) 420–424, https://doi.org/10.1038/nature17946.
[15] N.M. Gaudelli, A.C. Komor, H.A. Rees, M.S. Packer, A.H. Badran, D.I. Bryson, D. R. Liu, Programmable base editing of A•T to G•C in genomic DNA without DNA cleavage, Nature 551 (2017) 464–471, https://doi.org/10.1038/nature24644.
[16] C. Huang, G. Li, J. Wu, J. Liang, X. Wang, Identification of pathogenic variants in cancer genes using base editing screens with editing efficiency correction, Genome Biol. 22 (2021) 80, https://doi.org/10.1186/s13059-021-02305-2.
[17] J. Kweon, A.-H. Jang, H.R. Shin, J.-E. See, W. Lee, J.W. Lee, S. Chang, K. Kim, Y. Kim, A CRISPR-based base-editing screen for the functional assessment of BRCA1 variants, Oncogene 39 (2020) 30–35, https://doi.org/10.1038/s41388-019-0968-2.
[18] H. Li, T. Ma, J.R. Remsberg, S.J. Won, K.E. DeMeester, E. Njomen, D. Ogasawara, K.T. Zhao, T.P. Huang, B. Lu, G.M. Simon, B. Melillo, S.L. Schreiber, J. Lykke-Andersen, D.R. Liu, B.F. Cravatt, Assigning functionality to cysteines by base editing of cancer dependency genes, Nat. Chem. Biol. 19 (2023) 1320–1330, https://doi.org/10.1038/s41589-023-01428-w.
[19] M.A. Coelho, S. Cooper, M.E. Strauss, E. Karakoc, S. Bhosle, E. Gonçalves, G. Picco, T. Burgold, C.M. Cattaneo, V. Veninga, S. Consonni, C. Dinçer, S.F. Vieira, F. Gibson, S. Barthorpe, C. Hardy, J. Rein, M. Thomas, J. Marioni, E.E. Voest, A. Bassett, M.J. Garnett, Base editing screens map mutations affecting interferon-γ signaling in cancer, Cancer Cell 41 (2023) 288–303.e6, https://doi.org/10.1016/j.ccell.2022.12.009.
[20] A.K. Sangree, A.L. Griffith, Z.M. Szegletes, P. Roy, P.C. DeWeirdt, M. Hegde, A. V. McGee, R.E. Hanna, J.G. Doench, Benchmarking of SpCas9 variants enables deeper base editor screens of BRCA1 and BCL2, Nat. Commun. 13 (2022) 1318, https://doi.org/10.1038/s41467-022-28884-7.
[21] J. Li, J. Lin, S. Huang, M. Li, W. Yu, Y. Zhao, J. Guo, P. Zhang, X. Huang, Y. Qiao, Functional phosphoproteomics in cancer chemoresistance using CRISPR-Mediated base editors, Adv. Sci. (Weinh.) 9 (2022) 2200717, https://doi.org/10.1002/advs.202200717.
[22] R.E. Hanna, M. Hegde, C.R. Fagre, P.C. DeWeirdt, A.K. Sangree, Z. Szegletes, A. Griffith, M.N. Feeley, K.R. Sanson, Y. Baidi, L.W. Koblan, D.R. Liu, J.T. Neal, J. G. Doench, Massively parallel assessment of human variants with base editor screens, Cell 184 (2021) 1064–1080.e20, https://doi.org/10.1016/j.cell.2021.01.012.
[23] R. Cuella-Martin, S.B. Hayward, X. Fan, X. Chen, J.-W. Huang, A. Taglialatela, G. Leuzzi, J. Zhao, R. Rabadan, C. Lu, Y. Shen, A. Ciccia, Functional interrogation of DNA damage response variants with base editing screens, Cell 184 (2021) 1081–1097.e19, https://doi.org/10.1016/j.cell.2021.01.041.
[24] L.W. Koblan, J.L. Doman, C. Wilson, J.M. Levy, T. Tay, G.A. Newby, J.P. Maianti, A. Raguram, D.R. Liu, Improving cytidine and adenine base editors by expression optimization and ancestral reconstruction, Nat. Biotechnol. 36 (2018) 843–846, https://doi.org/10.1038/nbt.4172.
[25] P. Xu, Z. Liu, Y. Liu, H. Ma, Y. Xu, Y. Bao, S. Zhu, Z. Cao, Z. Wu, Z. Zhou, W. Wei, Genome-wide interrogation of gene functions through base editor screens empowered by barcoded sgRNAs, Nat. Biotechnol. (2021), https://doi.org/10.1038/s41587-021-00944-1.
[26] S. Zhu, Z. Cao, Z. Liu, Y. He, Y. Wang, P. Yuan, W. Li, F. Tian, Y. Bao, W. Wei, Guide RNAs with embedded barcodes boost CRISPR-pooled screens, Genome Biol. 20 (2019) 20, https://doi.org/10.1186/s13059-019-1628-0.
[27] E.J. Eaton, B.J. Wick, J.S. Chacón, A.J. Wang, M. Kluesner, J.T. Barnes, B. Kar, M. Wang, M.J. Johnson, J.G. Skeate, B.R. Webber, B.S. Moriarity, Adenine base editor for knockout of proteins: a practical guide from design to analysis with updated MultiEditRbatch, Mol. Ther. Nucleic Acids 37 (2026) 102908, https://doi.org/10.1016/j.omtn.2026.102908.
[28] X. Wang, Z. Liu, G. Li, L. Dang, S. Huang, L. He, Y. Ma, C. Li, M. Liu, G. Yang, X. Huang, F. Zhou, X. Ma, Efficient gene silencing by adenine base editor-mediated start codon mutation, Mol. Ther. 28 (2020) 431–440, https://doi.org/10.1016/j.ymthe.2019.11.022.
[29] P. Billon, E.E. Bryant, S.A. Joseph, T.S. Nambiar, S.B. Hayward, R. Rothstein, A. Ciccia, CRISPR-mediated base editing enables efficient disruption of eukaryotic genes through induction of STOP codons, Mol. Cell 67 (2017) 1068–1079.e4, https://doi.org/10.1016/j.molcel.2017.08.008.
[30] C. Kuscu, M. Parlak, T. Tufan, J. Yang, K. Szlachta, X. Wei, R. Mammadov, M. Adli, CRISPR-STOP: gene silencing through base-editing-induced nonsense mutations, Nat. Methods 14 (2017) 710–712, https://doi.org/10.1038/nmeth.4327.
[31] A.J. Levine, p53, the cellular gatekeeper for growth and division, Cell 88 (1997) 323–331, https://doi.org/10.1016/S0092-8674(00)81871-1.
[32] L.E. Romick-Rosendale, V.W.Y. Lui, J.R. Grandis, S.I. Wells, The Fanconi anemia pathway: repairing the link between DNA damage and squamous cell carcinoma, Mutat. Res. Fund Mol. Mech. Mutagen 743–744 (2013) 78–88, https://doi.org/10.1016/j.mrfmmm.2013.01.001.
[33] M.R. Lieber, The mechanism of double-strand DNA break repair by the nonhomologous DNA end-joining pathway, Annu. Rev. Biochem. 79 (2010) 181–211, https://doi.org/10.1146/annurev.biochem.052308.093131.